Robust state transfer in the quantum spin channel via weak measurement and quantum measurement reversal

Zhi He,[1] Chunmei Yao,[1] and Jian Zou[2]
[1]*College of Physics and Electronics, Hunan University of Arts and Science, Changde 415000, People's Republic of China*
[2]*School of Physics, Beijing Institute of Technology, Beijing 100081, People's Republic of China*
(Received 9 June 2013; published 31 October 2013)

Using the weak measurement (WM) and quantum measurement reversal (QMR) approach, robust state transfer and entanglement distribution can be realized in the spin-$\frac{1}{2}$ Heisenberg chain. We find that the ultrahigh fidelity and long distance of quantum state transfer with certain success probability can be obtained using proper WM and QMR, i.e., the average fidelity of a general pure state from 80% to almost 100%, which is almost size independent. We also find that the distance and quality of entanglement distribution for the Bell state and the general Werner mixed state can be obviously improved by the WM and QMR approach.

DOI: 10.1103/PhysRevA.88.044304 PACS number(s): 03.67.Hk, 05.50.+q, 42.50.Dv

Introduction. Recently, it was shown that weak measurement (WM) and quantum measurement reversal (QMR) can effectively suppress amplitude-damping decoherence for a single qubit [1–3]. In particular, weak measurements and reversal can greatly suppress the disentanglement dynamics of two qubits interacting with their own independent reservoirs [4–6]. More interestingly, the famous entanglement sudden death (ESD) [7] can be avoided by the WM and QMR [5]. Now the WM and QMR also have been widely applied to various aspects of quantum information processing. In Ref. [8], the authors used the WM and QMR to generate the concurrence of assistance from tripartite to bipartite entanglement. In Ref. [9], the authors investigated entanglement amplification via local weak measurements. In Ref. [10], the authors discussed the improvement the fidelity of teleportation through noisy channels using weak measurement and they utilized the standard state teleportation scheme, namely a pair of maximally entangled states serving as state transfer channel. Most of the abovementioned concerns are focused on the model of the qubit system interacting with the reservoir.

On the other hand, it is well known that quantum communication based on quantum spin chain has been first addressed in the seminal Ref. [11]. The author demonstrated that the quantum spin chain can be used as a channel for short-distance quantum communication. Then several methods and models of a perfect state transfer were suggested [12,13]. The long-distance state transfer is always an essential task in quantum information processing. We have not seen any report for the application of the WM and QMR in the quantum spin chain model.

In this Brief Report, we explore the WM and QMR approach to enhance state transfer and entanglement distribution in the spin-$\frac{1}{2}$ Heisenberg chain channel. By investigation, using the WM and QMR we find that the lowest and highest average fidelity $\bar{F}$ of the general pure state through the spin chain channel can attain 80% and close to 100%. More especially, we find that the optimal state transfer is almost size independent. Then we investigate the entanglement distributions of the Bell state and the Werner-mixed state in the spin chain channel and find that the distance and quality of entanglement distribution can obviously improved. In comparison with the scheme of Ref. [11], the WM and QMR approach indicates its potential usefulness in quantum information processing based on the spin chain.

The paper is organized as follows: We give the detailed scheme for state transfer and entanglement distribution based on the WM and QMR, followed by results and discussion. Finally, we give the conclusion of our results.

State transfer and entanglement distribution scheme. Before describing our scheme, we briefly review the WM and QMR approach. The WM can be performed by a device that indirectly monitors a qubit. If the device has no signal (namely, the null result case), the qubit was only partially collapsed and we let it evolve. If the device has signal, we discard the result. The corresponding map of the WM with strength p_1 on the qubit in the computational basis $\{|0\rangle,|1\rangle\}$ can also be written as $\begin{pmatrix} 1 & 0 \\ 0 & \sqrt{1-p_1} \end{pmatrix}$. The effect of WM is reduction of the weight of the excited state $|1\rangle$, so that the excited state $|1\rangle$ will undergo less influence of decoherence. Conversely, the corresponding map of the QMR with strength p_2 in the computational basis can also be represented as $\begin{pmatrix} \sqrt{1-p_2} & 0 \\ 0 & 1 \end{pmatrix}$. Thus, the effect of QMR is restoration of the weight of the excited state $|1\rangle$.

In what follows, we discuss state transfer and entanglement distribution in a linear, open-ended, spin-$\frac{1}{2}$ isotropic Heisenberg chain which locates in an uniform external magnetic field using weak measurements and reversal. The entire solution of the model can be found in Ref. [11], and the transition amplitude $f_{N,1}^N(t_0)$ is

$$f_{N,1}^N(t_0) = \sum_{m=1}^{N} a_m v_{m,N} \cos[\pi(m-1)/(2N)], \qquad (1)$$

where $a_1 = 1/\sqrt{N}$, $a_{m\neq 1} = \sqrt{2/N}$, $v_{m,N} = a_m \cos[\pi(m-1)(2N-1)/(2N)]e^{-iE_m t_0}$, and $E_m = 2B + 2J\{1 - \cos[\pi(m-1)/N]\}$. In the following discussions, by choosing the proper magnetic field B, the transition amplitude $f_{N,1}^N(t_0) = \langle N|e^{-it_0 H}|1\rangle$ is a real number, i.e., $\arg\{f_{N,1}^N(t_0)\} = 0$. It is worth mentioning that Bose has also pointed out that the effect of the spin chain can act as an amplitude-damping quantum channel. Therefore, the evolution of the input state $\rho_{\rm nin} = |\phi_1\rangle\langle\phi_1|$ can be represented by the sum

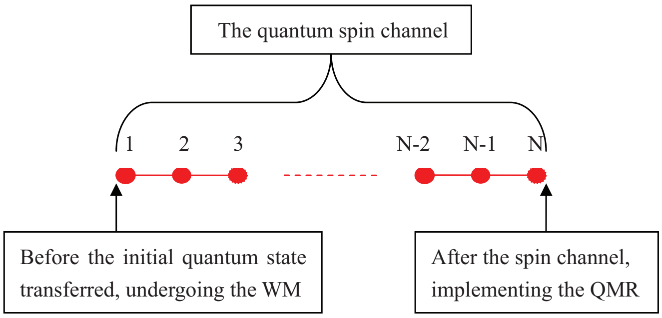

FIG. 1. (Color online) Schematic diagram of state transfer in spin chain by the WM and QMR.

of Kraus operators: $\rho_{\rm out} = M_0\rho_{\rm nin}M_0^\dagger + M_1\rho_{\rm nin}M_1^\dagger$, where $M_0 = \left(\begin{smallmatrix}1&0\\0&f\end{smallmatrix}\right)$, $M_1 = \left(\begin{smallmatrix}0&g\\0&0\end{smallmatrix}\right)$, and $f = |f^N_{N,1}(t_0)|$, $g = \sqrt{1-f^2}$.

Generally speaking, our scheme was divided into three steps as shown in Fig. 1: (1) Before going through the spin chain channel, the transferred initial quantum state was implemented with WM; (2) the quantum state of implementing the WM transfers in the spin chain channel; (3) after undergoing the spin chain channel in a reasonable time t_0, the QMR with strength p_2 was applied to the corresponding state.

Here, we assume that the general quantum state to be transferred initially prepared in $|\phi_{\rm in}\rangle = \cos(\theta/2)|0\rangle + e^{i\varphi}\sin(\theta/2)|1\rangle$ is located at the first spin of the total spin chain, while all the other spins are in the $|0\rangle$ state, where $|0\rangle$ and $|1\rangle$ denote the spin down and up states, respectively.

After the sequence of a WM with strength p_1 in first spin, spin chain channel, and QMR with strength p_2 in the Nth spin, the corresponding output state in Nth spin becomes

$$\rho_{\rm out} = \frac{1}{P_2}[(\alpha_1\sqrt{1-p_2}|0\rangle + \beta_1 f|1\rangle) \times(\alpha_1^*\sqrt{1-p_2}\langle 0| + \beta_1^* f\langle 1|) + (1-p_2)|\beta_1|^2g^2], \quad (2)$$

where $P_2 = (1-p_2)(1-f^2|\beta_1|^2) + f^2|\beta_1|^2$ is the total success probability of both the WM and QMR,

$$\alpha_1 = \frac{\cos(\theta/2)}{\sqrt{\cos^2(\theta/2) + (1-p_1)\sin^2(\theta/2)}} \quad (3)$$

and

$$\beta_1 = \frac{\sqrt{1-p_1}e^{i\varphi}\sin(\theta/2)}{\sqrt{\cos^2(\theta/2) + (1-p_1)\sin^2(\theta/2)}}. \quad (4)$$

If we have *a priori* knowledge about the magnitude of transition amplitude f, we can perform the optimal QMR with $p_2 = 1 + f^2(p_1 - 1)$ as pointed out in Refs. [1,3]. After employing the optimal QMR, the final output state can be obtained as

$$\rho_{\rm out}^{\rm opt} = \frac{T_p|\phi_{\rm in}\rangle\langle\phi_{\rm in}| + T_f|0\rangle\langle 0|}{T_p + T_f}, \quad (5)$$

where $T_p = (1-p_1)f^2$ and $T_f = \sin^2(\theta/2)(1-p_1)^2f^2g^2$. It is well known that the efficiency of a quantum state through the quantum spin channel can be measured by the average fidelity over all input states $|\phi_{\rm in}\rangle$ in the Bloch sphere, that is, $\bar{F}^{\rm opt} = (1/4\pi)\int\langle\phi_{\rm in}|\rho_{\rm out}^{\rm opt}(t_0)|\phi_{\rm in}\rangle d\Omega$ [14]. After some straightforward calculations, we obtain the explicit expression of the the average fidelity as

$$\bar{F}^{\rm opt} = \frac{1}{2} + \frac{1}{(1-p_1)(1-f^2)} - \frac{\ln[1+(1-p_1)(1-f^2)]}{(1-p_1)^2(1-f^2)^2}, \quad (6)$$

and the optimal success probability of both the WM and QMR,

$$P_2^{\rm opt} = \tfrac{1}{2}(1-p_1)f^2[2 + (1-p_1)(1-f^2)]. \quad (7)$$

Obviously, we can see that from Eq. (7) the optimal success probability $P_2^{\rm opt}$ is a monotonically decreasing function of p_1 for fixed f.

Furthermore, we study entanglement distribution in the same model using the WM and QMR. In what follows, we assume that a pair of particles A and B are initially in the extended Werner-like (EWL) mixed state, which has the form [15]

$$\rho(0) = \frac{1-r}{4}I + r|\Phi\rangle\langle\Phi|, \quad (8)$$

where r denotes the purity of the initial state and $|\Phi\rangle = \alpha|01\rangle + \sqrt{1-\alpha^2}|10\rangle$ is the Bell-like state with α real. It is obvious that the state given by Eq. (8) for $\alpha = 1/\sqrt{2}$ will reduce to the well-known Werner state [16], while for $r = 0$ and $r = 1$, the corresponding states become a totally mixed state and a well-known Bell state, respectively. Here, we assume that one of the pair of particles A and B, i.e., particle B is located in the first spin of the spin chain. It is obvious that the particle A and the Nth spin (because of particle B transferred to the Nth spin by free evolution) will establish entanglement.

Similar to the above discussion for the state transfer case, before and after through a spin chain we implement the WM in the first spin and QMR in the Nth spin, respectively. We finally can derive the final state in the computational basis $\{|00\rangle,|01\rangle,|10\rangle,|11\rangle\}$,

$$\rho_{\rm AN}(t_0) = \begin{pmatrix}\rho_{11} & 0 & 0 & 0\\ 0 & \rho_{22} & \rho_{23} & 0\\ 0 & \rho_{23} & \rho_{33} & 0\\ 0 & 0 & 0 & \rho_{44}\end{pmatrix}, \quad (9)$$

where the elements of the density matrix $\rho_{11} = \eta_{11}/P_4$, $\rho_{22} = \eta_{22}/P_4$, $\rho_{33} = \eta_{33}/P_4$, $\rho_{44} = \eta_{44}/P_4$, $\rho_{23} = \eta_{23}/P_4$ correspond to other parameters given by $\eta_{11} = (1-p_4)[1-r+(1-f^2)(1-p_3)(1-r+4r\alpha^2)]/4$, $\eta_{22} = f^2(1-p_3)(1-r+4r\alpha^2)/4$, $\eta_{33} = (1-p_4)[2-p_3-f^2(1-p_3)(1-r)+2r+p_3r-4r\alpha^2]/4$, $\eta_{44} = f^2(1-p_3)(1-r)/4$, $\eta_{23} = fr\sqrt{1-p_3}\sqrt{1-p_4}\alpha\sqrt{1-\alpha^2}$. The total success probability of the both WM with strength p_3 and QMR with strength p_4 is defined as

$$P_4 = \{2(1-p_4) + (1-r+2r\alpha^2) \times[p_4f^2(1-p_3) - p_3(1-p_4)]\}/2. \quad (10)$$

The concurrence for $\rho_{\rm AN}(t_0)$ given by Eq. (9) can be expressed as [17,18]

$$C_{\rm AN}(p_3,t_0,p_4) = 2{\rm Max}\{0,|\rho_{23}| - \sqrt{\rho_{11}\rho_{44}}\}, \quad (11)$$

The exact expression for the concurrence is too cumbersome and is not reported here.

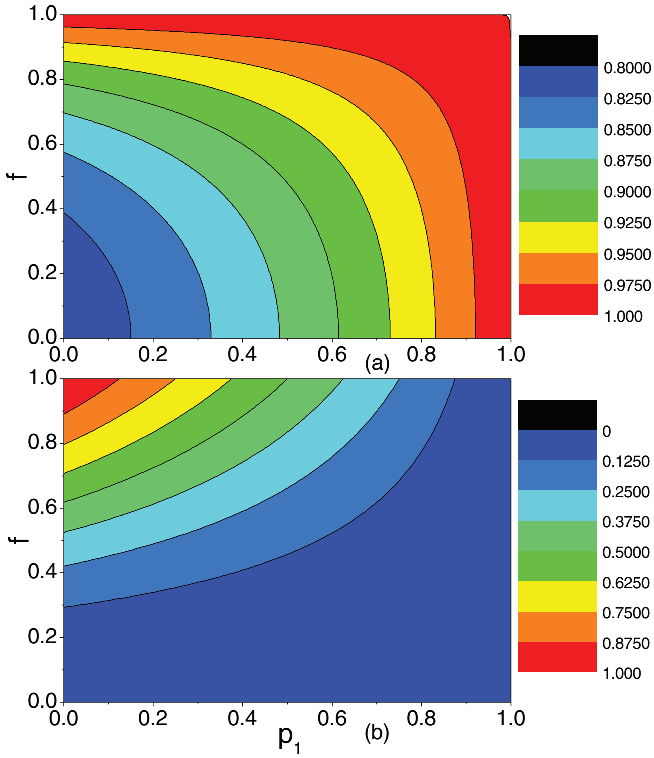

FIG. 2. (Color online) The optimal average fidelity $\bar{F}^{\rm opt}$ (a) and success probability $P_2^{\rm opt}$ (b) as functions of the transition amplitude f and the WM strength p_1.

Results and discussion. First, we consider state transfer by means of the WM and QMR. In light of Eqs. (6) and (7), we plot the average fidelity $\bar{F}^{\rm opt}$ and total success probability $P_2^{\rm opt}$ as functions of the transition amplitude f and the WM strength p_1 as shown in Fig. 2. From Fig. 2(a), we can clearly see that the average fidelity $\bar{F}^{\rm opt}$ always will exceed the highest fidelity $F = 2/3$ of classical transmission of a quantum state for any $f \neq 0$ and p_1. More interestingly, the lowest average fidelity can also reach 80% for the small WM strength p_1 and the highest average fidelity $\bar{F}^{\rm opt}$ will be close to 1 for the large p_1. However, the higher fidelity comes at the expense of the success probability, as shown in Fig. 2(b). Moreover, from Fig. 2 it is easy to see that as the WM strength p_1 is larger, the the state transfer is also larger for each transition amplitude f, but this is the reverse for the success probability. There is hence a tradeoff between success probability and the average fidelity, such that the desirable value of p_1 depends on the practical consideration. The general conclusion of the tradeoff between information gain and reversibility in weak measurement was proved in Ref. [19], which is one of distinct features of weak measurement. We calculate the average fidelity $\bar{F}^{\rm opt}$ and success probability $P_2^{\rm opt}$ for some p_1 and fixed $f = 0.5$; i.e., when $p_1 = 0.1$, $\bar{F}^{\rm opt} = 0.849$ and $P_2^{\rm opt} = 0.301$; when $p_1 = 0.6$, $\bar{F}^{\rm opt} = 0.918$ and $P_2^{\rm opt} = 0.115$.

We also numerically calculate the average fidelity $\bar{F}^{\rm opt}$ for some spin length N_L with the WM and QMR for fixed $p_1 = 0.2$ and $p_1 = 0.99$ and without control in Table I. Throughout this report the time interval $t \in [0,4000/J]$, which is the same as in Ref. [11]. First we consider a small $p_1 = 0.2$ case as shown in Table I and find that the average fidelity $\bar{F}^{\rm opt}$ is more than 80% for longer spin chain. Then we also consider the average fidelity $\bar{F}^{\rm opt}$ for large $p_1 = 0.99$ as shown in Table I and find that almost perfect state transfer for longer spin chain can be realized. In Ref. [11], the author pointed out that the average fidelity of a general pure state will exceed the highest fidelity for a classical transmission of a quantum state until the chain length N is larger than 80. Here, from Table I we can clearly see that in our scheme the average fidelity $\bar{F}^{\rm opt} \approx 99.7\%$ but with certain success probability for $N = 8 \times 10^3$ and $p_1 = 0.99$. More especially, the high average fidelity is almost size independent. Then we also calculate the average fidelity without control. From Table I, we can find that the average fidelities with the WM and QMR are always more than 2/3 while the average fidelities without control are always less than 2/3 for large spin number. Now the success probability for large spin number may be not too high. However, from the above discussion we can learn that the WM and QMR approach in enhancing the average fidelity of state transfer through the spin chain channel is very useful.

TABLE I. The average fidelity $\bar{F}^{\rm opt}$ for different spin chain length N_L with the WM and QMR for fixed $p_1 = 0.2$ and $p_1 = 0.99$ and $\bar{F}$ without control. The results are obtained in a time interval $t \in [0,4000/J]$, which is the same as in Ref. [11].

N_L	5×10^2	1×10^3	2×10^3	5×10^3	8×10^3	
$\bar{F}^{\rm opt}$	0.835	0.834	0.833	0.832	0.832	$p_1 = 0.2$
$\bar{F}^{\rm opt}$	0.997	0.997	0.997	0.997	0.997	$p_1 = 0.99$
$\bar{F}$	0.561	0.548	0.538	0.527	0.515	without control

On the other hand, we discuss entanglement distribution by means of the WM and QMR approach. It is obvious that the state given by Eq. (8) for $\alpha = 1/\sqrt{2}$, $r = 1$ will reduce to the Bell state. According to Eqs. (10) and (11), we plot the concurrence $C_{\rm AN}$ (a) and success probability P_4 (b) as the WM strength p_3 and the QMR strength p_4 for the Bell state as shown in Fig. 3. The other parameter is the transition amplitude $f = 0.170$, namely for $N = 500$. From Fig. 3(a), we can clearly see that $C_{\rm AN}$ is a monotonically increasing function of p_4 for fixed f and p_3, but this is the reverse for the success probability P_4 as shown in Fig. 3(b). Then we can also see that from Fig. 3 that the both $C_{\rm AN}$ and P_4 are a monotonically decreasing function of p_3 for fixed f and p_4. In order to obtain the better concurrence $C_{\rm AN}$ and success probability P_4, we need to choose the proper p_3 and p_4. We calculate the concurrence $C_{\rm AN}$ and success probability P_4 for some cases, i.e., when $p_3 = 0.1$ and $p_4 = 0.7$, $C_{\rm AN} = 0.301$ and $P_4 = 0.294$; when $p_3 = 0.1$ and $p_4 = 0.9$, $C_{\rm AN} = 479$ and $P_4 = 0.107$.

Furthermore, we also concretely list the concurrence $C_{\rm AN}$ for some spin length N_L with the WM and QMR for fixed $p_3 = 0.1$ and $p_4 = 0.9$ and without control in Table II. Table II shows that the entanglement distribution $C_{\rm AN}$ can still maintain high entanglement through longer spin chain. When compared with Ref. [11], in which the entanglement is 0.135 for $N = 1000$, in our scheme the entanglement can reach 0.396 with certain success probability for the same spin number. In sum, the WM and QMR can strongly suppress decoherence for

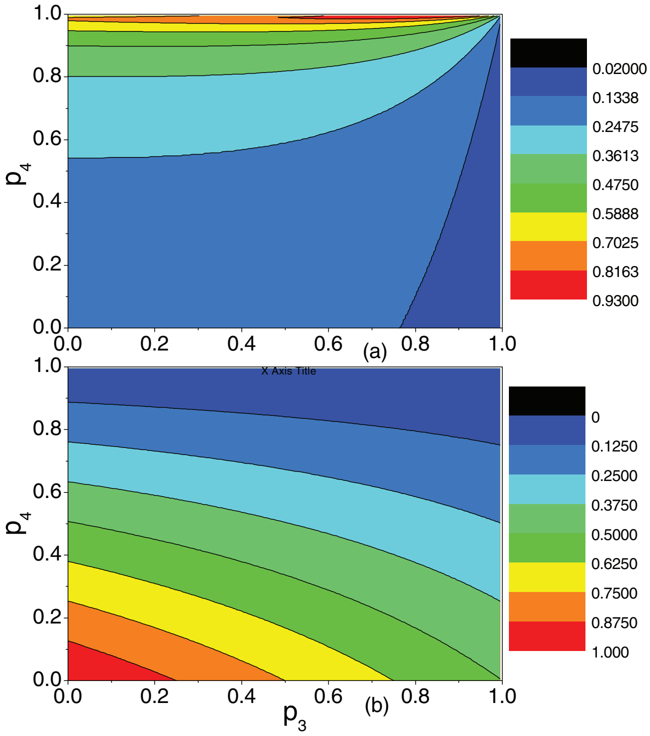

FIG. 3. (Color online) The concurrence $C_{\rm AN}$ (a) and success probability P_4 (b) as the WM strength p_3 and the QMR strength p_4 for the Bell state. The other parameter is the transition amplitude $f = 0.170$, namely for $N = 500$, and the time interval is the same as in Table I.

the entanglement distribution of the pure state in spin chain channel. Then we also calculate entanglement distribution for a general Werner mixed state, namely letting $\alpha = 1/\sqrt{2}, r = 0.8$ in Eq. (8). We find that the WM and QMR approach is also very effective.

Conclusions. In conclusion, we have studied the WM and QMR approach to realize robust state transfer and entanglement distribution through the spin-$\frac{1}{2}$ Heisenberg channel by means of the WM and QMR. We found that the average

TABLE II. The concurrence $C_{\rm AN}$ for different spin chain lengths N_L with the WM and QMR for fixed $p_3 = 0.1$ and $p_4 = 0.9$ and $\bar{C}_{\rm AN}$ without control. The time interval are the same as in in Table I.

N_L	5×10^2	1×10^3	2×10^3	5×10^3	8×10^3	
$C_{\rm AN}$	0.479	0.396	0.322	0.243	0.140	with control
$\bar{C}_{\rm AN}$	0.170	0.135	0.107	0.079	0.045	without control

fidelity of state transfer and entanglement distribution can be obviously enhanced by the WM and QMR. This investigation has indicated that the WM and QMR have potential usefulness in quantum information processing based on spin chain model although the WM and QMR are a probabilistic approach. Here, it is worth stating that the spin-$\frac{1}{2}$ Heisenberg chain can act as an amplitude-damping quantum channel, as pointed out in Ref. [11], which is the reason why the WM and QMR approach can be employed to enhance state transfer and entanglement distribution in the spin chain. The idea of manipulating spin chain by the WM and QMR can also be applied to the case of two parallel Heisenberg spin chains, which will be an interesting topic. As for the current experimental development for the WM and QMR to suppress amplitude-damping decoherence, we can refer to Ref. [5], which implements protection of entanglement of photons subjected to amplitude-damping decoherence using the WM and QMR. In addition, some spin chain models can be theoretically and experimentally simulated in trapped ions [20,21], coupled quantum dots [22], ultracold quantum gases [23], and Josephson junctions [24]. Therefore, we hope that the scheme proposed may be tested by experimental setup in the near future.

Acknowledgments. This work is financially supported by the National Science Foundation of China (Grants No. 61144006, No. 11274043, and No. 11247294), the Project Fund of Hunan Provincial Science and Technology Department (Grant No. 2010FJ3147), the Research Foundation of Education Bureau of Hunan Province, China (Grant No. 12C0826), the Doctor Foundation Startup from Hunan University of Arts and Science (Grant No. 13101039), and Hunan Province Key Laboratory of Photoelectric Information Integration and Optical Manufacturing Technology.

[1] A. N. Korotkov and K. Keane, Phys. Rev. A **81**, 040103(R) (2010).
[2] Y. S. Kim, Y. W. Cho, Y. S. Ra, and Y. H. Kim, Opt. Express **17**, 11978 (2009).
[3] J. C. Lee, Y. C. Jeong, Y. S. Kim, and Y. H. Kim, Opt. Express **19**, 16309 (2011).
[4] Q. Sun, M. Al-Amri, L. Davidovich, and M. S. Zubairy, Phys. Rev. A **82**, 052323 (2010).
[5] Y.-S. Kim, J.-C. Lee, O. Kwon, and Y.-H. Kim, Nat. Phys. **8**, 117 (2012).
[6] Z. X. Man, Y. J. Xia, and N. B. An, Phys. Rev. A **86**, 012325 (2012).
[7] T. Yu and J. H. Eberly, Phys. Rev. Lett. **93**, 140404 (2004).
[8] C. Yao, Z. H. Ma, Z. H. Chen, and A. Serafini, Phys. Rev. A **86**, 022312 (2012).
[9] Y. Ota, S. Ashhab, and F. Nori, J. Phys. A **45**, 415303 (2012).
[10] T. Pramanik and A. S. Majumdar, arXiv:1301.0281v2 [quant-ph].
[11] S. Bose, Phys. Rev. Lett. **91**, 207901 (2003).
[12] M. Christandl, N. Datta, A. Ekert, and A. J. Landahl, Phys. Rev. Lett. **92**, 187902 (2004).
[13] N. Y. Yao *et al.*, Phys. Rev. Lett. **106**, 040505 (2011).
[14] M. A. Nielsen and I. L. Chuang, *Quantum Computation and Quantum Information* (Cambridge University Press, Cambridge, 2000).
[15] B. Bellomo, R. Lo Franco, and G. Compagno, Phys. Rev. A **77**, 032342 (2008).
[16] R. F. Werner, Phys. Rev. A **40**, 4277 (1989).
[17] W. K. Wootters, Phys. Rev. Lett. **80**, 2245 (1998).
[18] T. Yu and J. H. Eberly, Quantum Inf. Comput. **7**, 459 (2007).

[19] Y. W. Cheong and S. W. Lee, Phys. Rev. Lett. **109**, 150402 (2012).
[20] A. M. Childs and I. L. Chuang, Phys. Rev. A **63**, 012306 (2000).
[21] R. Blatt and C. F. Roos, Nat. Phys. **8**, 277 (2012).
[22] D. Loss and D. P. DiVincenzo, Phys. Rev. A **57**, 120 (1998).
[23] I. Bloch, J. Dalibard, and S. Nascimbene, Nat. Phys. **8**, 267 (2012).
[24] L. H. Du, X. Zhou, Y. J. Han, G. C. Guo, and Z. W. Zhou, Phys. Rev. A **86**, 032302 (2012).